

AN OPTICAL TRACKING APPROACH TO COMPUTER-ASSISTED SURGICAL NAVIGATION VIA STEREOSCOPIC VISION

Darin Tsui¹, Capalina Melentyev¹, Ananya Rajan¹, Rohan Kumar¹, Frank E. Talke¹

¹Center for Memory and Recording Research
University of California, San Diego, San Diego, CA, USA, 92093

ABSTRACT

Computer-assisted surgical navigation has become a popular solution in difficult operations where a high amount of precision is required. Current state-of-the-art methods of surgical navigation involve tracking reflective 3D marker spheres using IR stereoscopic cameras. However, the cost of implementing such systems may not be affordable for smaller healthcare systems. In this paper, we propose that fully optical navigation has the potential to be a viable alternative to state-of-the-art reflective marker navigation. We use fiducial ArUco markers to facilitate the tracking of real-time position. Using two inexpensive cameras, we design and calibrate a stereoscopic camera to record the 3D position of an ArUco marker moving through space. A positioning platform was developed to assess the position predicted from the stereoscopic camera to the real-life position of the marker. Additionally, we explore the possibility of using different color spaces and physical marker colors to improve the detection percentage and accuracy of markers. We identified that black-and-white ArUco markers using the Hue, Saturation, and Lightness (HSL) color space gave a mean error of 5.3 mm. Black-and-white ArUco markers using the Red, Green, and Blue (RGB) color space gave the highest detection percentage. In the future, the mean error can be reduced by increasing the camera quality, and by using a multi-stereoscopic camera setup.

Keywords: surgical navigation, computer-assisted surgery, stereoscopic vision, fiducial ArUco markers, homography

NOMENCLATURE

d	disparity
f	focal length
b	baseline distance between two cameras
h_{ij}	homography value at position (i,j)
x_i	X camera coordinate at position i
x_i	X world coordinate at i

1. INTRODUCTION

In recent years, surgical navigation systems have seen usage in many medical fields, including neurosurgery, orthopedic, and maxillofacial surgeries [1]. One of the main reasons for the implementation of such navigation systems is their ability to provide real-time guidance to surgeons during invasive and minimally invasive procedures [2]. As such, current state-of-the-art navigation systems are able to provide surgeons with high precision, thus improving the success of the surgery [3].

Existing approaches to surgical navigation revolve around the usage of infrared (IR) stereoscopic cameras [3]. In this approach, retro-reflective markers are made visible to near-infrared stereoscopic cameras [4]. Although these systems are reliable, they are expensive. On the other hand, fully optical, or videometric tracking, uses a calibrated camera to track patterned markers. This technology is more accessible to healthcare institutions due to its low cost [5]. In this paper, we propose that the use of stereoscopic, videometric tracking with fiducial markers has the potential to be a low cost alternative in surgical navigation.

2. METHODS

2.1 Stereoscopic Camera Setup

To establish that optical marker tracking is a promising alternative to traditional surgical navigation systems, we developed an inexpensive tracking system, as seen in Fig. 1, using off-the-shelf parts. For 3D positional tracking, we calibrated a stereoscopic camera system using two web cameras (HZQDLN HD). At the time of this publication, these cameras retail for \$40. This sets the total cost of the stereoscopic system significantly cheaper compared to other state-of-the-art navigation systems. Figure 2 displays our stereo camera setup. The distance between the two cameras is 72 mm.

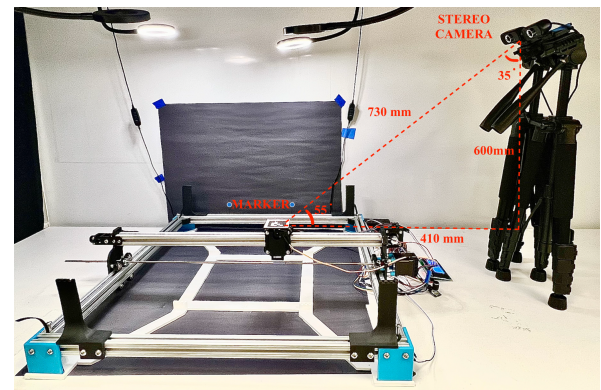


FIGURE 1: EXPERIMENTAL SETUP OF THE STEREOSCOPIC CAMERA RELATIVE TO THE POSITIONING PLATFORM.

We calibrated our stereoscopic camera system using an 8 by 11 calibration checkerboard, in accordance with calibration checkerboard documentation [6]. OpenCV was used to obtain

intrinsic camera parameters, which includes the focal length and optical centers.



FIGURE 2: STEREOSCOPIC CAMERA SETUP.

2.2 Marker Tracking Implementation

We implemented the ArUco marker package through OpenCV to facilitate positional tracking. ArUco markers are part of a square-based fiducial marker system that specializes in camera pose estimation [7]. The ArUco markers are created with a binary matrix that facilitates marker identification. As the ArUco marker moves in space, the stereoscopic camera tracks the center position of the marker. Given the centers of the ArUco marker as seen by the two cameras, we can compute the disparity between the markers. The disparity, d , is defined as the difference in horizontal position between the left and right cameras.

$$d = x_l - x_r \quad (1)$$

With the focal length, f , and baseline distance, b , of the camera and the disparity, we are able to compute the 3D position of the marker using equations (2-4).

$$z = \frac{fb}{d} \quad (2)$$

$$x = \frac{x_z}{f} \quad (3)$$

$$y = \frac{y_z}{f} \quad (4)$$

2.3 Experimental Setup

To test the accuracy of the stereo camera and positioning algorithm on moving markers, we developed a positioning platform to move the marker in the X and Y directions. Figure 3 displays the positioning platform used. The positioning platform uses two motors to move the marker in a square pattern. In our experiments, the moving marker was shuttled around following the pattern shown in Fig. 4.

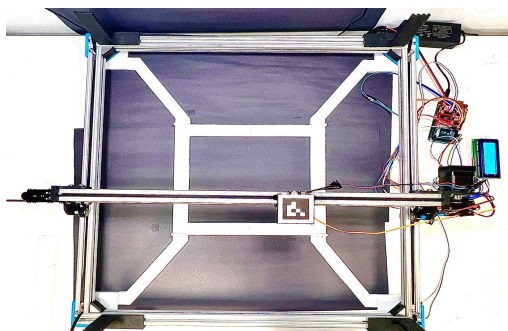


FIGURE 3: POSITIONING PLATFORM SETUP. THE MOVING MARKER IS ABLE TO MOVE IN THE X AND Y DIRECTIONS.

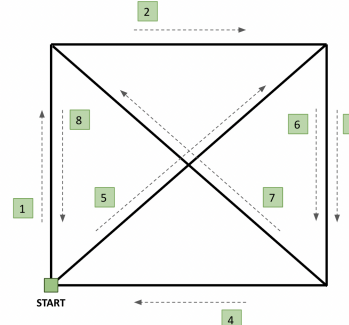


FIGURE 4: MARKER MOVEMENT PATTERN, DISPLAYING THE ORDER OF MOVEMENT.

During experiments, we placed our stereo camera on a tripod a distance of 410 mm away from the center of the marker's starting point. The stereo camera captured the moving marker at a 35 degree angle at a height of 680 mm. Light of intensity 37 lux was provided by a ring LED. Figure 1 displays the complete setup of the experiment.

2.4 Marker Tracking Experiments

To integrate optical tracking into surgical navigation, it is important to explore the parameters that would best optimize the reliability and accuracy of navigation. For this paper, we explore two parameters: color space conversion and the marker's physical color.

In all marker tracking experiments, the ArUco marker was moved at a speed of 20 mm/sec. The markers used for these experiments had a width of 40mm and a pixel density of 4x4. The pixel density is defined as the number of bits, or inner squares, of the ArUco marker. Three trials were performed for all experiments.

2.4.1 Color Space Conversions and Marker Color

Upon capturing live video of the marker moving on the positioning platform, we converted the video frames to different color spaces. Marker tracking tests were performed in Red, Green, and Blue (RGB), Hue, Saturation, and Lightness (HSL), and Hue, Saturation, and Value (HSV) color spaces. These three spaces were chosen, as they are the most commonly used color spaces in image processing. When converting from RGB to HSL or HSV, thresholding was performed on the output. In HSL, the lower threshold for Lightness (L) was chosen to be 50%. In HSV, the lower threshold for Value (V) was set to 55%. Hue and Saturation remained the same.

Additionally, we also varied the color of the actual ArUco marker to see if that would have an impact in the different color spaces. We tested white, pink, yellow, and orange-colored markers, as seen in Fig. 5.



FIGURE 5: COLORED ArUCO MARKERS THAT WERE TESTED ON.

2.5 3D Mapping Verification of Marker Position

Upon obtaining the 3D position of the marker from the stereo camera's perspective, we evaluated the positional accuracy of the camera by projecting the marker's position from camera coordinates to real-world coordinates. To do this, we transformed the 3D coordinates of the markers onto the XY plane using the corners of the marker movement square. From here, homography was performed on the X and Y coordinates to convert the marker coordinates of the camera to real-life distances. The coordinates used to perform homography were taken from the corners of the marker movement square. Equation (5) details the calculation of the homography matrix. Here, h_{ij} represents the homography value at position (i,j) .

$$\begin{bmatrix} x_1 & y_1 & 1 & 0 & 0 & 0 & -x_1x'_1 & -y_1x'_1 \\ 0 & 0 & 0 & x_1 & y_1 & 1 & -x_1y'_1 & -y_1y'_1 \\ x_2 & y_2 & 1 & 0 & 0 & 0 & -x_2x'_2 & -y_2x'_2 \\ 0 & 0 & 0 & x_2 & y_2 & 1 & -x_2y'_2 & -y_2y'_2 \\ x_3 & y_3 & 1 & 0 & 0 & 0 & -x_3x'_3 & -y_3x'_3 \\ 0 & 0 & 0 & x_3 & y_3 & 1 & -x_3y'_3 & -y_3y'_3 \\ x_4 & y_4 & 1 & 0 & 0 & 0 & -x_4x'_4 & -y_4x'_4 \\ 0 & 0 & 0 & x_4 & y_4 & 1 & -x_4y'_4 & -y_4y'_4 \end{bmatrix} \begin{bmatrix} h_{11} & h_{12} & h_{13} \\ h_{21} & h_{22} & h_{23} \\ h_{31} & h_{32} & h_{33} \end{bmatrix} = \begin{bmatrix} x'_1 \\ y'_1 \\ x'_2 \\ y'_2 \\ x'_3 \\ y'_3 \\ x'_4 \\ y'_4 \end{bmatrix} \quad (5)$$

After computing the homography matrix, the camera coordinates were converted to real-life distances using equation (6), where x_m and y_m are the camera coordinates of the moving marker. Following the conversion to real-life distances, the error was calculated by comparing the real-life distance the marker moves to the distance the marker moves in world coordinates.

$$\begin{bmatrix} x' \\ y' \\ 1 \end{bmatrix} \approx \begin{bmatrix} h_{11} & h_{12} & h_{13} \\ h_{21} & h_{22} & h_{23} \\ h_{31} & h_{32} & h_{33} \end{bmatrix} \begin{bmatrix} x_m \\ y_m \\ 1 \end{bmatrix} \quad (6)$$

3. RESULTS AND DISCUSSION

3.1 Results

To determine the reliability of the optical tracking system, we report our results in terms of detection percentage. To calculate this, we compared the total amount of frames captured to the amount of times the marker was able to be detected as it moved along its premeditated path.

Table 1 reports the detection percentage observed when tracking the moving marker in different color spaces and marker colors.

Table 1. DETECTION PERCENTAGE (%) OF FOUR COLORED MARKERS IN RGB, HSL AND HSV COLOR SPACES.

Color Space	Color			
	White	Pink	Yellow	Orange
RGB	99.7	98.1	97.1	99.5
HSL	99.5	81.3	89.7	87
HSV	97.5	73.5	78.4	80.6

It is evident that the RGB colorspace performs best for all marker colors. Additionally, when comparing the colors, it can be seen that the white marker consistently had the best accuracy out of the 4 colors tested.

Table 2 reports the mean error across all three trials when tracking the moving marker in different color spaces and marker colors.

Table 2: MARKER TRACKING AVERAGE ERROR (MM) OF FOUR COLORED MARKERS IN RGB, HSL, AND HSV COLOR SPACES.

Color Space	Color			
	White	Pink	Yellow	Orange
RGB	5.48	5.62	12.35	5.37
HSL	5.38	6.80	5.96	6.26
HSV	5.61	6.98	6.17	5.88

From the results shown in Table 2, it is evident that the white colored marker in the HSL colorspace performs the best.

3.2 Discussion

Based on the results in Section 3.1, the development of a fully optical surgical navigation system is promising. While the mean error of the system is higher than would be needed for clinical use, the fact that the stereoscopic system was created using inexpensive, off-the-shelf parts demonstrates the potential of such a system with further optimization.

To reduce the error of the system, several improvements could be implemented. For one, recreating the stereoscopic system with higher quality cameras would improve the accuracy of the system, as well as increase the marker detection percentage regardless of the color space and marker color used. Additionally, designing a multi-stereoscopic camera system would likely improve detection and accuracy of the system over a single stereoscopic camera. From here, one could find the position of the marker by taking a weighted average of the two camera positions depending on which camera is closer to the marker.

4. CONCLUSION

In this study, we have designed and calibrated a stereoscopic camera to record the 3D position of a moving ArUco marker. We explored the accuracy and detection percentage of the ArUco marker by varying color spaces and the marker's physical color. A positioning platform was used to evaluate the accuracy of the stereoscopic system. Using black-and-white ArUco markers in the HSL color space, we obtained a mean error of 5.3 mm.

ACKNOWLEDGEMENTS

Research towards this project was supported by the UCSD General Campus Research Senate Grant #2019201.

REFERENCES

- [1] Zhang, Mengshi, Bo Wu, Can Ye, Yu Wang, Juan Duan, Xu Zhang, and Nan Zhang. 2019. "Multiple Instruments Motion Trajectory Tracking in Optical Surgical Navigation." *Optics Express* 27 (11): 15827. <https://doi.org/10.1364/oe.27.015827>.
- [2] Contreras López, William Omar, Paula Alejandra Navarro, and Santiago Crispin. 2019. "Intraoperative Clinical Application of Augmented Reality in Neurosurgery: A Systematic Review." *Clinical Neurology and Neurosurgery* 177 (February): 6–11. <https://doi.org/10.1016/j.clineuro.2018.11.018>.
- [3] Mezger, Uli, Claudia Jendrewski, and Michael Bartels. 2013. "Navigation in Surgery." *Langenbeck's Archives of Surgery* 398 (4): 501–14. <https://doi.org/10.1007/s00423-013-1059-4>.
- [4] Wu, Han, Qinyong Lin, Rongqian Yang, Yuan Zhou, Lingxiang Zheng, Yueshan Huang, Zhigang Wang, Yonghua Lao, and Jinhua Huang. 2019. "An Accurate Recognition of Infrared Retro-Reflective Markers in Surgical Navigation." *Journal of Medical Systems* 43 (6). <https://doi.org/10.1007/s10916-019-1257-x>.
- [5] Sorrento, Angela, Maria Bianca Porfido, Stefano Mazzoleni, Giuseppe Calvosa, Miria Tenucci, Gastone Ciuti, and Paolo Dario. 2020. "Optical and Electromagnetic Tracking Systems for Biomedical Applications: A Critical Review on Potentialities and Limitations." *IEEE Reviews in Biomedical Engineering* 13: 212–32. <https://doi.org/10.1109/rbme.2019.2939091>.
- [6] Zhengyou Zhang. 2004. "Camera Calibration with One-Dimensional Objects." *IEEE Transactions on Pattern Analysis and Machine Intelligence* 26 (7): 892–99. <https://doi.org/10.1109/tpami.2004.21>.
- [7] Garrido-Jurado, S., R. Muñoz-Salinas, F.J. Madrid-Cuevas, and M.J. Marín-Jiménez. 2014. "Automatic Generation and Detection of Highly Reliable Fiducial Markers under Occlusion." *Pattern Recognition* 47 (6): 2280–92. <https://doi.org/10.1016/j.patcog.2014.01.005>.